Soft Matter

RSC Publishing

PAPER

View Article Online
View Journal | View Issue

Morphological transition of self-assembled architectures from PEG-based ether-anhydride terpolymers

Cite this: *Soft Matter*, 2013, **9**, 3021

Tao Chen,†[a] Xing Guo,†[a] Aijun Zhao,[a] Jie Wang,[a] Chunli Shi[b] and Shaobing Zhou*[ab]

Biodegradable micelles were fabricated by self-assembly in the aqueous solution of PEG-based ether-anhydride terpolymer consisting of poly(ethylene glycol) (PEG), 1,3-bis(*p*-carboxyphenoxy) propane (CPP) and sebacic acid (SA). Morphological transition of the micelles was investigated in terms of PEG chain length, hydrophilic–hydrophobic segment ratio, polymer concentration and environmental temperature. The effect of micellar shape on drug loading capacity and cytotoxicity was evaluated. The cellular uptake efficiency was characterized qualitatively with the human hepatoblastoma cell lines (HepG2) and fibroblast normal cells by fluorescence microscopy. Primary *in vivo* biodistribution of the drug-loaded micelles with diverse morphologies in tumor and normal tissues was also assessed using 4T1 bearing mice. The results show that terpolymer micelles with rod-like shape possess better biocompatibility and the *in vivo* biodistribution is dependent on micellar shape. Therefore, these polymer micelles have great potential as a novel drug vehicle in nanomedicine.

Received 20th September 2012
Accepted 20th November 2012

DOI: 10.1039/c2sm27173g

www.rsc.org/softmatter

Introduction

Molecular self-assembly technology is capable of producing intermolecular complexes *via* controlling their primary, secondary, tertiary, and quaternary structures; typical examples include peptides and nucleic acids.[1] Molecular self-assembly has also been employed to produce intricate bio-inspired nanostructures from synthetic block copolymers in dilute solution, which may eventually be matched with natural biological structures in sophistication and precision.[1] To the best of our knowledge, very limited progress has been made in the comparison between these synthetic nanostructures and their natural counterparts.

Polymeric micelles are emerging as promising nanocarriers for drug delivery with many advantages, including small size (10–200 nm), enhanced permeability, high structural stability, and improved solubility and bioavailability for hydrophobic drugs.[2–8] They are formed usually by either hydrophobic interactions that exist between hydrophobic blocks such as polylactide,[9] polycaprolactone[10] and polyacrylamides,[11] or electrostatic interactions[12] which induce the self-assembly of amphiphilic block copolymers into core–shell structures. Recently, some endeavors have been made in the self-assembly behavior of amphiphilic polymers. It has been found that the amphiphilic polymers may form similar structures as their low-molecular-weight counterparts in some special solvents.[13] Besides of the common spherical core–shell structure, micelles can also be worm-like, rod-like, tubed, lamellar shape and ordered microporous films. It is generally believed that macromolecular surfactants offer important advantages over conventional low-molecular-weight amphiphilies.[14]

It is worth noting that morphology impacts the micellar stability, capability of loading drug, release properties, as well as *in vivo* pharmacokinetics and biodistribution.[15–19] Worm-like polymeric micelles, bio-inspired by filovirus that infects human cells, have been attracting great interest as a new drug delivery carriers.[15–19] It is reported that the worm-like micelles could load and solubilize twice as much hydrophobic paclitaxel as spherical micelles consisting of the same block copolymer;[17] flexible filomicelles are not rapidly cleared and instead appear to circulate longer than spherical nanoassemblies composed of very similar PEG based diblock copolymers;[16] worm-like micelles or rod-like micelles consisting of PLLA-*b*-PEG display slower DOX release behaviors compared to spherical micelles.[20] Therefore, micellar shape is a crucial parameter influencing the characteristics and performance in drug delivery.

Morphogenesis of amphiphilic block copolymers in aqueous media have been extensively studied.[21–25] However, amphiphilic triblock copolymers or terpolymers have received less attention than the diblock counterparts. Recent studies show that they can also assemble into complex architectures.[26]

[a]*Key Laboratory of Advanced Technologies of Materials, Ministry of Education, School of Materials Science and Engineering, Southwest Jiaotong University, Chengdu, 610031, P. R. China. E-mail: shaobingzhou@swjtu.cn; shaobingzhou@hotmail.com; Fax: +86-28-87634649; Tel: +86-28-87634023*

[b]*School of Life Science and Engineering, Southwest Jiaotong University, Chengdu, 610031, P. R. China*

† Co-first Author.

The capability to change the morphology in a controlled manner is of great interest due to the potential advantages and applications of nonspherical aggregates in the field of drug delivery. In this study, we extend our investigation to the design and synthesis of biodegradable amphiphilic PEG-based ether-anhydride terpolymers *via* melt polycondensation. In contrary to the CPP and SA chains comprising the hydrophobic blocks, PEG is chosen as the hydrophilic block in the backbone of amphiphilic poly(PEG : CPP : SA) terpolymers. The amphiphilic terpolymers can self-assemble into polymeric micelles with a colloidal size in aqueous solution. The PEG outer shell is considered a critical factor in the reduction of micelle uptake by the mononuclear phagocyte system (MPS).[27] In addition, the hydrophobic polyanhydride (CPP and SA) possess favorable biodegradability and biocompatibility.[28] To our knowledge, the amphiphilic terpolymer is firstly used for fabricating micelles with different morphologies. The morphology of micelles in aqueous solution is controlled by altering the length of PEG chains, hydrophilic–hydrophobic ratio, concentration of polymer in solution and environmental temperature. In particular, the effect of these morphologies on the drug-loading, the cellular uptake *in vitro* and biodistribution *in vivo* was also investigated.

Experimental section

Materials

Succinic anhydride, sebacic acid (SA), acetic anhydride, poly(ethylene glycol) (PEG, M_n = 2, 4, 8 kDa), 1,3-dibromopropane, *p*-hydroxybenzoic acid were obtained from Chengdu KeLong Chemical Reagent Company (Sichuan, Chengdu, China). Before use, succinic anhydride was refluxed over and distilled from magnesium; SA was recrystallized twice from ethanol. All other solvents were used as received without further purification. 1,3-Bis-(carboxyphenoxy) propane (CPP) was synthesized by the method described in ref. 29. The PEG-based ether-anhydride terpolymers were synthesized *via* melt-condensation polymerization without catalyst.[28] Human liver carcinoma cell lines (HepG2) were purchased from Sichuan University (China). Doxorubicin hydrochloride (DOX·HCl) was purchased from Zhejiang Hisun Pharmaceutical Co., Ltd (China).

Micellization

The polymeric micelles were prepared using a precipitation method.[30] First, preweighed poly(PEG_{4000} : CPP : SA) (20 : 20 : 60) terpolymers and DOX·HCl (0.1 mg) were dissolved in a mixture of 4.9 mL tetrahydrofuran (THF) and 0.1 mL water; the solution obtained was then added dropwise into 10 mL deionized water using a disposable syringe (21 gauge) and stirred for 4 h at room temperature to facilitate the removal of THF. Once the THF had been removed completely, the drug-loaded micelles were transferred into a dialysis bag (MWCO 8000–12 000) with distilled water to remove the unloaded DOX·HCl. Drug-loaded micelles were gathered by lyophilisation.

Characterization

The morphology of micelles was characterized by atomic force microscopy (AFM; Tapping mode; CSPM5000, Being, China). The samples were prepared by casting dilute micelles solution on a silicon piece, which were then dried under vacuum. The morphology of micelles was also observed with a Transmission electron microscope (TEM) (Hitachi H-700H, Japan) at an acceleration voltage of 150 kV. The mean size and size distribution were determined by Zeta sizer, MALVERN Nano-ZS90 (Malvern Ltd., Malvern, UK) in water at room temperature. All data were averaged over three measurements. By using a UV-vis spectrophotometer (UV-2550, Shimadu, Japan), drug-loading efficiency was determined from the ratio of the weight of DOX·HCl in micelles to the total amount of DOX·HCl. Drug-loading content was determined from the ratio of the weight of DOX·HCl loaded to that of the micelles.

In vitro cytotoxicity study

The cytotoxicity of blank micelles with different morphologies was evaluated using an MTT assay. The HepG2 tumor cells were planted at a density of 5×10^3 cells per well in 500 μL of medium in 48-well plates and grown for 48 h. The cells were then exposed to a series of polymeric micelles with different morphologies (rod-like, worm-like and spherical) for 48 h. Finally, the plates were read in an automated microplate spectrophotometer (ELX800 Biotek, USA) at 570 nm as reference. The same tests were performed as mentioned above every 24 h until 48 h. All data were expressed as the mean ±S.D.

The effect of micelle morphology on cellular uptake

For qualitative cellular uptake analysis, HepG2 cells were seeded into 12-well plates at 5×10^4 cells per well with 2 mL RPMI 1640 medium. The cells were kept in the incubator at 37 °C in humidified atmosphere containing 5% CO_2. After incubation for 24 h, worm-like, rod-like and spherical micelles loaded 5 μg mL^{-1} DOX·HCl were added. After incubation for the predetermined time, the medium in the testing wells was removed and the wells were washed with PBS three times to remove the micelles outside of the cells. Afterwards the cells were fixed with 2.5% glutaraldehyde for 30 minutes and then the cell nuclei were stained with 4′,6-diamidino-2-phenylindole (DAPI, blue) for three minutes. The procedure for the normal cells, fibroblast, cultured with the three types of micelles was similar as mentioned above. A fluorescence microscope (Olympus IX51, Japan) was used to observe the cellular uptake of DOX·HCl-loaded micelles with different morphologies.

The effect of micelle morphology on biodistribution *in vivo*

DOX·HCl was used as a fluorescent indicator for the pharmacokinetics and biodistribution studies. Murine breast cancer cell 4T1 (2×10^5 cells) were inoculated into female Balb/c mice (6–7 weeks, 20 ± 2 g) subcutaneously in the right back of mice, and the tumor was allowed to reach a volume of about 50 mm^3. 24 mice were divided into four groups randomly and injected *via* the tail vein with free DOX·HCl and DOX·HCl-loaded

micelles with spherical (S), rod-like (R) and worm-like (W) shapes at an equivalent DOX·HCl dose of 5 mg kg^{-1}. After 6 h and 24 h respectively, the predetermined mice were sacrificed, tumors and normal organs, *i.e.* liver, heart, spleen, lung and kidney were excised and collected (12 mice at each time point) and immediately frozen in liquid nitrogen until further analysis.

For the qualitative evaluation, fluorescence microscopy (Olympus IX51, Japan) was used to visualize the accumulation of DOX·HCl in tumor cryo-sectioned at 5–7 μm thickness. For the quantitative measuring, the organs frozen in liquid nitrogen were weighed and pestled. DOX·HCl distributed in tumors and other tissues were extracted using DMSO solvent, and then the mixtures were separated by centrifugation at 5000 rpm for 30 min. The concentration of DOX·HCl in the supernatant was measured using a UV-vis spectrophotometer (UV-2550, Shimadzu, Japan) by the UV absorption at 482 nm.

Results and discussion

Most recently, micelles with tailored shape and size are paid more and more attention for the production of well-defined nano-objects. To study the micelle morphology is very important because the morphology influences their application as nanocarriers in drug delivery systems.[31] In this work, the micellization is carried out by a self-assembly method based on the amphiphilic poly(PEG : CPP : SA) terpolymers whose chemical structure was investigated in detail as our previous report.[32] The real weight ratios of PEG, SA and CPP blocks in the terpolymers calculated from ^{1}H NMR are 17.6 : 18.9 : 63.5, 26.7 : 18.7 : 54.6 and 36.1 : 19.5 : 44.4 for poly(PEG_{4000} : CPP : SA) with PEG_{4000}–CPP–SA segment ratios of 20 : 20 : 60, 30 : 20 : 50 and 40 : 20 : 40, respectively. The molecular weight (M_w) is 63 kDa, 50 kDa and 41 kDa, and corresponding polydispersity index is 2.23, 1.96 and 1.72 for poly(PEG_{4000} : CPP : SA) with PEG_{4000}–CPP–SA segment ratios of 20 : 20 : 60, 30 : 20 : 50 and 40 : 20 : 40, respectively. We have demonstrated the trigger of morphological transitions in aqueous solution not only by changing the polymer structure but also by altering the concentration of the terpolymer and the environmental temperature.

Characterization of the function of the PEG chain length

Although diblock copolymers are the most popular promoters of micelles, ABC triblock copolymers or terpolymer deserve interest because of the higher complexity of the generated nanostructures.[33] From Fig. 1, it can be seen that the morphology of these micelles can be controlled by changing the length of the hydrophilic PEG chains. At the same concentration in aqueous solution, poly(PEG_{2000} : CPP : SA) (20 : 20 : 60) terpolymer tends to assemble into the various non-spherical structures, while poly(PEG_{4000} : CPP : SA) (20 : 20 : 60) cannot do it. Different rod-like micelles can be found from poly(PEG_{2000} : CPP : SA) (20 : 20 : 60) terpolymer as shown in Fig. 1a–c. The formation mechanism of the rod-like micelles in our system remains unclear although we believe that adhesive contact and fusion of micelles are involved. As exhibited in Fig. 1c and e, the morphology of micelles is rod-like and spherical, respectively, whereas the aggregates transform into coexistence of worm-like and spherical micelles in Fig. 1d. The average diameter of the worm-like and spherical micelles is almost the same, and worm-like micelles may be associated by spherical ones. The rod-like micelles also formed from these spherical micelles as shown in Fig. 1c. Because it can be found many spherical nodes in the rod-like micelles, and the diameter of the rod is also the same with that of spherical micelles. One possible mechanism involves adhesive collisions and repeated aggregation of the spherical micelles to form the worm-like or rod-like micelles.[34] In addition, the worm-like micelles are the re-assembly of spherical micelles. The free energy balance from forming such rod-like aggregates determined the micelle morphology.

Fig. 1k–o show the AFM images of the micelles fabricated from the poly(PEG_{8000} : CPP : SA) (20 : 20 : 60). It can be found that at all concentrations most micelles have spherical morphology, due to the longer PEG chains of poly(PEG_{8000} : CPP : SA) (20 : 20 : 60) than poly(PEG_{2000} : CPP : SA) (20 : 20 : 60). For PEG-based ether-anhydride amphiphilic terpolymer, the longer the PEG chain, the more contribution to the overall free energy there is. The spherical micelles rather than other types of micelles tend to be formed when the PEG chain is longer.[24] Therefore, it can be concluded that terpolymer with shorter PEG chains could assemble easily into micelles with more diverse morphologies.

The TEM images in Fig. 2 further confirm the micellar structure. It can be also observed that the morphologies of micelles at the concentration of 1.0, 2.0 and 8.0 mg mL^{-1} are worm-like, rod-like and spherical, respectively, as shown in Fig. 2.

Characterization of the function of the hydrophilic–hydrophobic segment ratio

Fig. 3 shows the AFM images of the micelles prepared from poly(PEG_{4000} : CPP : SA) terpolymers with PEG–CPP–SA weight ratios of 30 : 20 : 50 and 40 : 20 : 40 at different concentrations. The morphology of all micelles formed from poly(PEG_{4000} : CPP : SA) (40 : 20 : 40) are spherical at every concentration as shown in Fig. 3d–f. The diameters of the spherical micelles are in the range of 70–120 nm. The reason may be ascribed to an increase of hydrophilicity in the terpolymer. Because water-soluble blocks are relatively long, it is inclined to form spherical micelles. However, the diameter of the spherical micelles decreases with the increasing concentration of polymer. The reason can be attributed to the increasing interactions among macromolecules as the concentration increases which makes the PEG chains curl and shrink.

For poly(PEG_{4000} : CPP : SA) (30 : 20 : 50), worm-like micelles are formed at 1.0 mg mL^{-1} (Fig. 3b). As shown in Fig. 1f and h, 3b and e, the micellar morphologies of poly(PEG_{4000} : CPP : SA) terpolymers change from spherical to rod-like with increasing the ratio of CPP and SA segments, while spherical micelles occur at all different concentrations for the terpolymer with

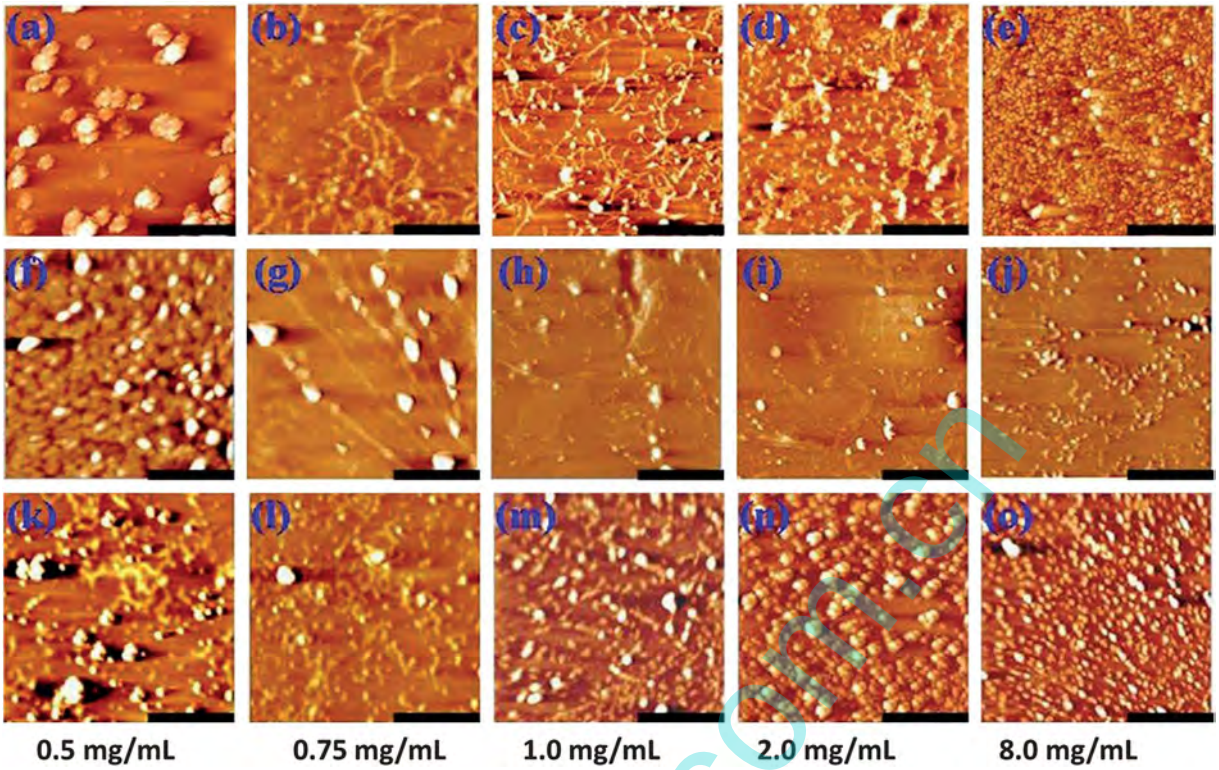

Fig. 1 AFM images of poly(PEG : CPP : SA) (20 : 20 : 60) micelles with PEG_{2000} (a–e), PEG_{4000} (f–j) and PEG_{8000} (k–o) at the concentrations of 0.5, 0.75, 1.0, 2.0 and 8.0 mg mL^{-1} (all scale bars are 2 μm).

PEG–CPP–SA weight ratio of 40 : 20 : 40. The free energy of aggregation is affected by the inter-coronal chain interaction, the core-coronal interfacial energy and the degree of core-chain stretching. Here, these polymeric micelle characters are capable of forming specific interactions *via* self-association through the hydrophilic–hydrophobic balance and thus the hydrophilic–hydrophobic segment ratio plays an important role in determining the morphology of the micellar corona. This can be qualitatively explained by Vilgis theory.[35] The folding amount of CPP and SA increases with the hydrophobic CPP and SA segments expanding, thus the diameter of micellar core increases. Consequently, it makes the space occupied by PEG chains in micellar corona larger, which leads to a decrease of interaction among macromolecular chains within corona. Additionally, the process is not favorable to entropy change, so the micellar morphology will transform if the environmental condition is suitable.[35]

Characterization of the function of the polymer concentration

We studied the effect of polymer concentration on micelle morphological transition by fixing the composition of terpolymer and only altering the PEG chains length. Fig. 1a–e show the AFM images of the micelles formed from poly-(PEG_{2000} : CPP : SA) (20 : 20 : 60) at different concentrations in water. Rod-like and spherical micelles can be observed in Fig. 1a. At the low concentration, the rod-like micelle is more stable than the spherical micelle. For decreasing the free energy

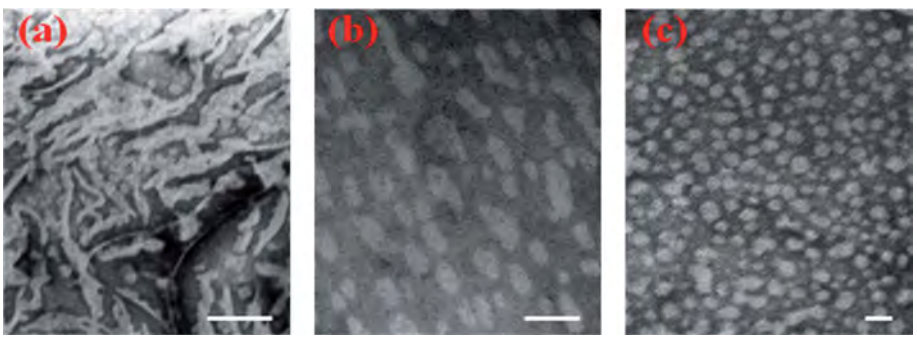

Fig. 2 TEM images of poly(PEG_{2000} : CPP : SA) (20 : 20 : 60) micelles at the concentration of 1.0 (a), 2.0 (b) and 8.0 (c) mg mL^{-1} (all scale bars are 200 nm).

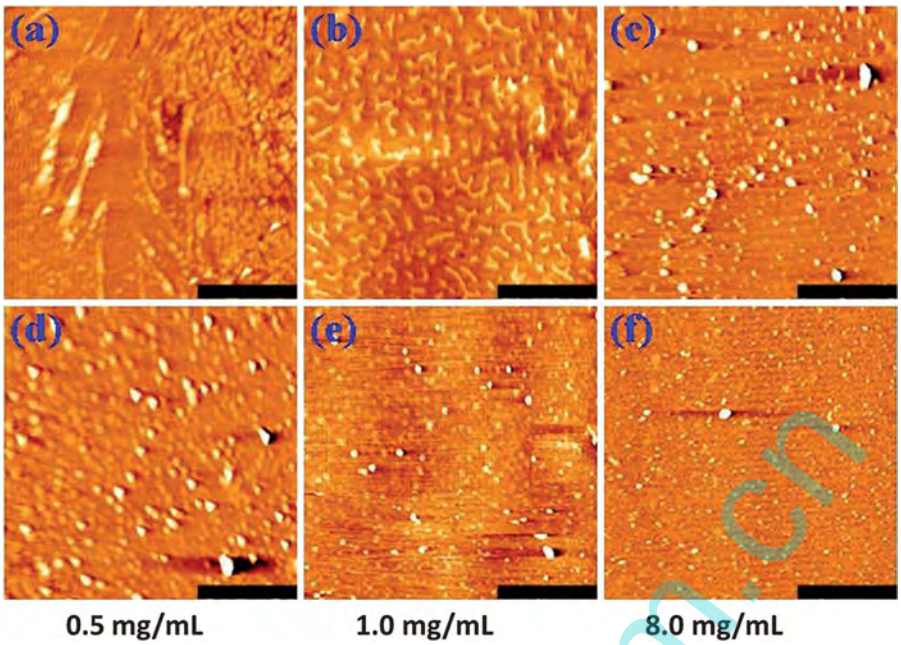

Fig. 3 AFM images of poly(PEG_{4000} : CPP : SA) micelles with PEG_{4000}–CPP–SA segment ratios of 30 : 20 : 50 (a–e) and 40 : 20 : 40 (d–f) at the concentrations of 0.5, 1.0 and 8.0 mg mL^{-1} (all scale bars are 2 μm).

of aggregation, the spherical micelles reassemble other morphologies. With increasing the concentration, complex morphologies become longer and tend to transform to rod-like, corresponding to the shapes in Fig. 1b–d. When the polymer concentration reaches 4.0 mg mL^{-1}, all micelles change to uniform spherical structure as shown in Fig. 1e. For the micelles formed from poly(PEG_{4000} : CPP : SA) (20 : 20 : 60) (Fig. 1f–j) and poly(PEG_{8000} : CPP : SA) (20 : 20 : 60) (Fig. 1k–o), the effect of the polymeric concentration on morphological transitions is almost similar to that of poly(PEG_{2000} : CPP : SA) (20 : 20 : 60), and the concentration at which the rod-like micelles transform to spherical micelles decreases with increasing PEG chain length. The range of polymer concentration to form rod-like micelle becomes wider, and the value of highest concentration to obtain rod-like micelles is increased.

To further demonstrate the influence of polymer concentration on micellar morphological transition clearly, we also focused on studying the morphologies of poly(PEG_{4000} : CPP : SA) micelles. As displayed in Fig. 3, poly(PEG_{4000} : CPP : SA) terpolymers have the same tendency of morphological transition as a function of the concentration. Large numbers of studies have emphasized on the morphology of aggregates formed from amphipathic copolymers whose hydrophobic blocks are longer than the hydrophilic blocks.[25] Morphological transition from rod-like to worm-like and then to spherical micelles can be seen in Fig. 2a–c. Fig. 3a shows the coexistence of rod-like and spherical structures when the terpolymer concentration is 0.5 mg mL^{-1}, the diameter of rod-like micelle is the same with that of spherical micelles but the length is 20–50 times longer than their diameter. At 1.0 mg mL^{-1} of the terpolymer concentration (Fig. 3b) the worm-like micelles were formed. The worm-like micelles have the same cross-sectional structure as the spherical micelles, but their length can reach up to a bigger scale and often possess a branched or randomly networked structure. At 8.0 mg mL^{-1}, only spherical micelles (Fig. 3c) can be observed with an average diameter of 120 nm. These changes usually occur with the decrease of the polymer concentration, resulting from the decrease of repulsive force. The reason was discussed in Eisenberg and Shen's report.[36] With increasing water content in the micelle solution, the solvent tends to be poorer to dissolve the core-forming CPP and SA segments, thus the interfacial tension increases, while the corona interaction may not change too much since both THF and water are good solvents for the corona-forming PEG segment.[36] The influences of the interfacial tension and the repulsion are contrary but the core chain stretching plays a key role in micellar transition. Therefore, the change from rod-like to worm-like and to spherical shape is a result of stressing the stretching of polymer chains in the core.[36]

Characterization of the function of the temperature of micelle solution

As deionized water added into micellar solution, the change in temperature of the system has an effect on the polymer–solvent interaction parameters.[37] In our previous report, we find that the PEG-based ether-anhydride terpolymers micelles solution displayed an excellent thermo-sensitive property.[38] The morphological transition with increasing temperature is also investigated as shown in Fig. 4a. Spherical micelles formed from poly(PEG_{4000} : CPP : SA) are observed at 4.0 mg mL^{-1}, and temperature increase results in a morphological transition from spherical to short rod-like (Fig. 4f and j) to an aggregation of the

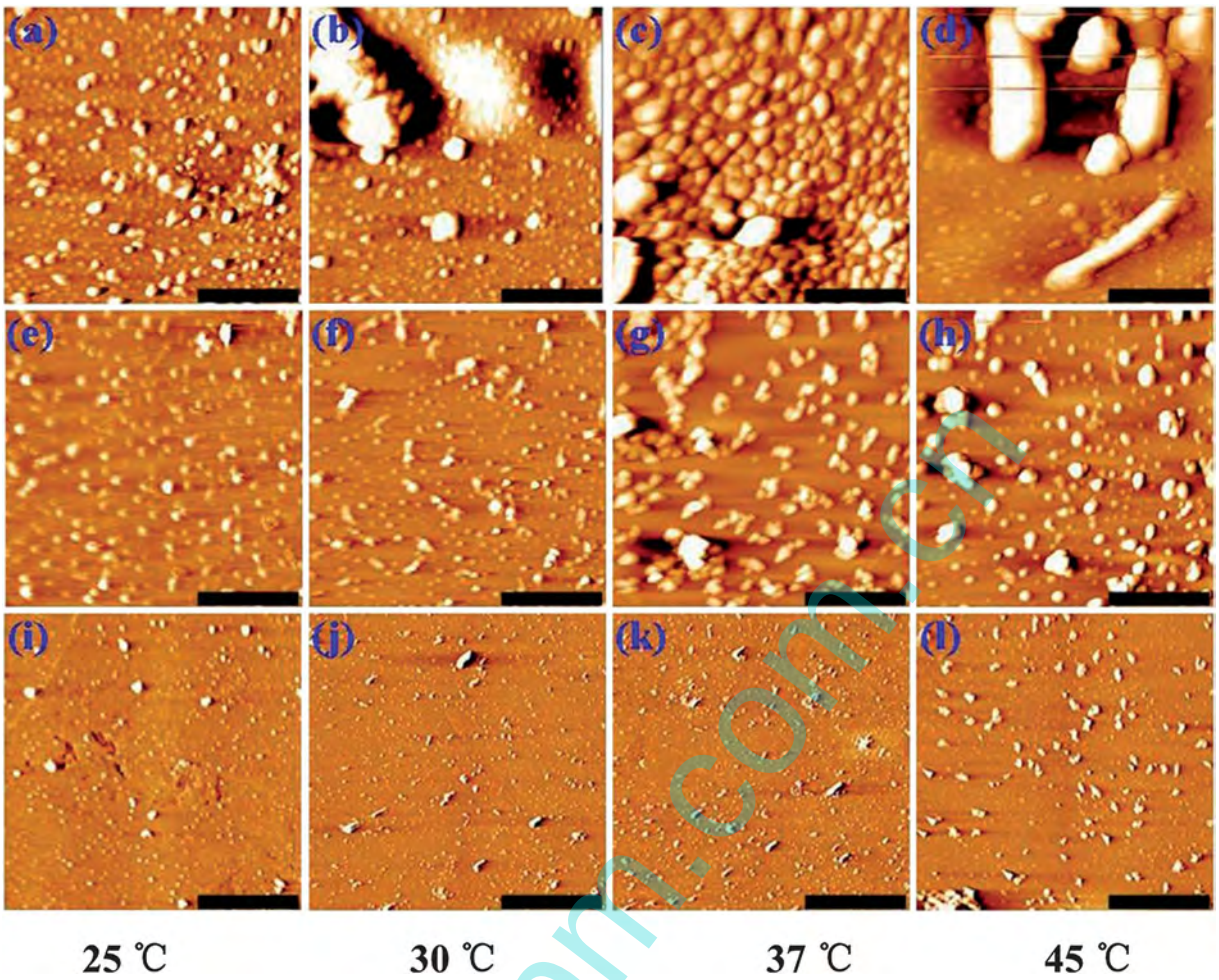

Fig. 4 AFM images of poly(PEG_{4000} : CPP : SA) micelles with PEG_{4000}–CPP–SA segment ratios of 20 : 20 : 60 (a–d), 30 : 20 : 50 (e–h) and 40 : 20 : 40 (i–l) at the concentration of 4.0 mg mL^{-1} at 25 °C, 30 °C, 37 °C and 45 °C, respectively (all scale bars are 2 μm).

micelles (Fig. 4c, g and l). The thermo-responsive transition is mainly influenced by the structure of the amphiphilic terpolymer. The thermo-responsive transition of micelles from poly(PEG_{4000} : CPP : SA) (20 : 20 : 60) is more obvious and the micrometer-sized granules are obtained at 45 °C (Fig. 4d). Such a temperature-dependent morphological transition is coincident with the thermo-sensitive phase transition of poly(PEG_{4000} : CPP : SA) micelles as studied previously.[38] When the temperature is below the cloud point, the polymeric micelles are randomly suspended in aqueous solution. During the thermo-sensitive transition, the hydrophilic PEG chains as surrounding corona of the micelles shrink at the initial stage of heating because of the dehydration, and then connect together to form the larger aggregates driven by the intermicellar hydrophobic interaction.[39] The micelle diameter obtained by DLS and the morphological transition were controlled by the temperature.[40] To sum up, individual primary micelles tend to combine together (intermicellar aggregation) gradually with increasing solution temperature, and the tendency to form combined micelles is stronger for poly(PEG_{4000} : CPP : SA) with higher weight ratio of CPP and SA.

The diameter of poly(PEG_{4000} : CPP : SA) (20 : 20 : 60) micelles increases and the size distribution becomes more extensive at elevated temperatures as shown in Fig. 5a–c. However, poly(PEG_{4000} : CPP : SA) (40 : 20 : 40) micelles are more stable, which is attributed to its higher hydrophilicity. The increase of the temperature results in the increases in the *Z*-average diameter of the micelles because of the aggregation of micelles. Fig. 5d displays the average diameter changes of micelles formed from poly(PEG_{4000} : CPP : SA) with PEG content of 20%, 30% and 40% in their aqueous solution (4.0 mg mL^{-1}) as a function of temperature. The diameters increase from 90 to 220 nm and from 120 to 400 nm for poly(PEG_{4000} : CPP : SA) (40 : 20 : 40) and poly(PEG_{4000} : CPP : SA) (20 : 20 : 60), respectively, as temperature increased from 25 °C to 55 °C. The cloud point of poly(PEG_{4000} : CPP : SA) (20 : 20 : 60) and poly(PEG_{4000} : CPP : SA) (30 : 20 : 50) micelle solution at 4.0 mg mL^{-1} is 33.5 °C and 37.5 °C, respectively, whereas no cloud point was observed for poly(PEG_{4000} : CPP : SA) (40 : 20 : 40) micelle solution due to its higher hydrophilicity.[38] The stable micelles from the terpolymers could be obtained due to the hydrophilic–hydrophobic balance in aqueous solution below

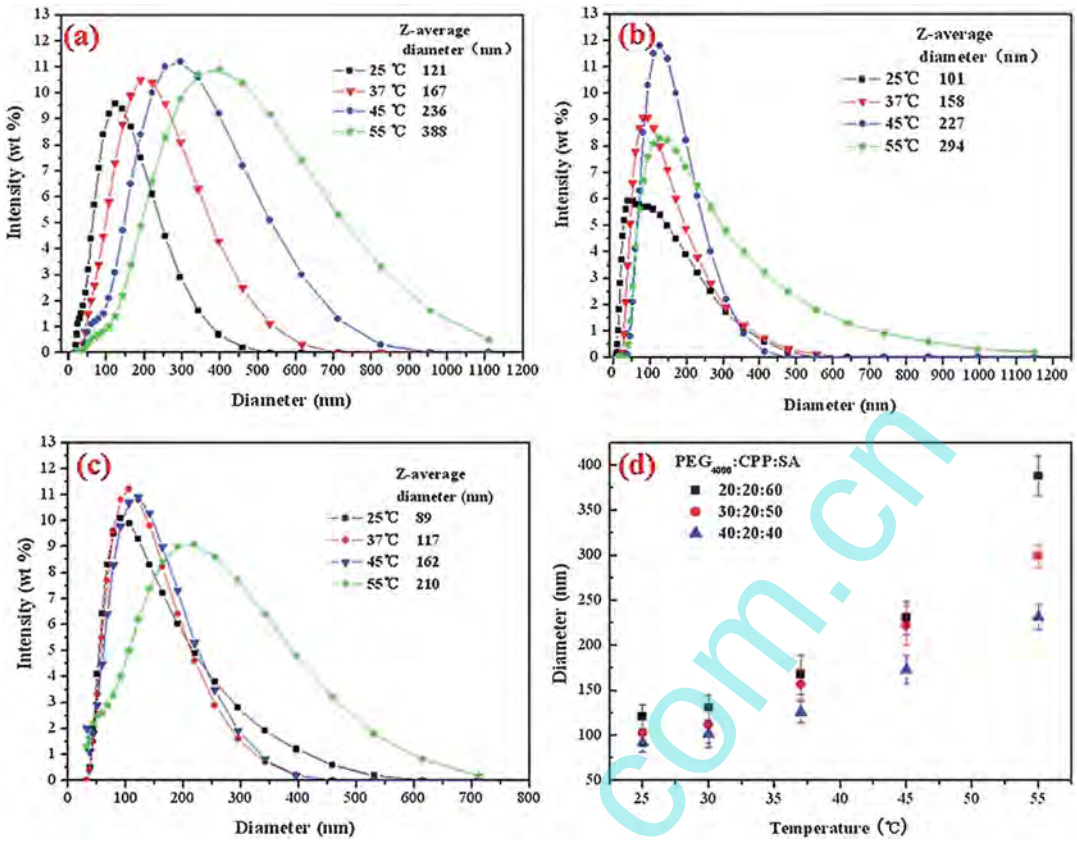

Fig. 5 Micellar size distribution of poly(PEG_{4000} : CPP : SA) micelles with PEG_{4000}–CPP–SA segment ratios of 20 : 20 : 60 (a), 30 : 20 : 50 (b) and 40 : 20 : 40 (c) at the concentration of 4.0 mg mL^{-1}, and diameter changes as a function of temperature (d).

the cloud point. The result is in agreement with our previous report that the hydrophilic–hydrophobic balance of the thermo-responsive terpolymers is a critical factor to make micelles stable.[41]

The effect of the micelle morphologies on drug-loading efficiency

The drug-loaded micelles could be self-assembled in aqueous solution from the amphiphilic terpolymers as illustrated in Fig. 6. The various morphologies (rod-like, worm-like and spherical) of DOX·HCl-loaded micelles formed from poly(PEG_{4000} : CPP : SA) (20 : 20 : 60) were controlled by altering the polymer concentrations. The micelle morphology has a great impact on its drug loading efficiency as summarized in Table 1. The amount of DOX·HCl (0.1 mg) added is very small compared with the polymer mass (20 mg), resulting in the low loading amount. Therefore, herein we only use the drug loading efficiency to discuss the impact of morphology. For the rod-like micelles, the DOX·HCl loading efficiency is 81.2%. With the morphology changing, the drug loading efficiency is reduced. For the spherical micelles, the DOX·HCl loading efficiency is the lowest (70.5%). In our previous report, we find that the DOX·HCl is encapsulated in the micelle core and partially adsorbed on micelle surface.[38] Thus, the higher drug loading efficiency and loading content would be contributed to the larger core volume (per carrier) and the more cavities of the aggregation (rod-like micelles).

In vitro cytotoxicity study

The MTT assay was performed to evaluate the toxicity of terpolymers micelles with different morphologies in order to investigate whether micelle morphology influences the viability

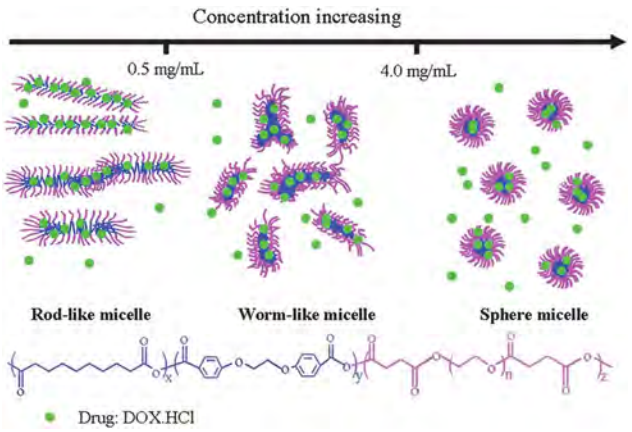

Fig. 6 A mechanism for the self-assembly of the drug-loaded poly(PEG_{4000} : CPP : SA) (20 : 20 : 60) micelles as a function of concentration.

Table 1 Characteristics of micelles with different morphologies

Morphology	Drug/polymer	Polymer concentration in water (mg mL^{-1})	Size (nm)	PDI	Drug-loading efficiency (%)	Drug-loading content (%)
Rod-like	0.1/20	0.5	235	0.279	81.2 ± 1.8	0.40 ± 0.06
Worm-like	0.1/20	1.0	153	0.253	72.3 ± 1.5	0.36 ± 0.03
Spherical	0.1/20	8.0	123	0.231	70.5 ± 1.5	0.35 ± 0.04

of the HepG2 tumor cells (Fig. 6a). The polymeric micelles with various morphologies at different concentrations significantly influence the growth of the HepG2 tumor cells. At the same concentration, cell viability in a group treated with spherical micelles is the lowest, whereas the highest cell viability is for the group treated with rod-like micelles. It is speculated that the nonspherical micelles can disrupt flow in the vasculature or be difficult for cellular internalization.[15] According to the MTT assay in Fig. 7a, it also can be found that the micelles at the concentration of 1.0 mg mL^{-1} with diverse shapes display slight cytotoxicity compared to the control group. Secondly, the difference of cell viability for these micelles was reduced by the 2nd day. It was demonstrated that these nonspherical micelles could transform into spherical micelles, which was driven by hydrolytic degradation of the CPP and SA by an "end-cleavage" mechanism.[42] The mean size decreases gradually during the transition from the rod-like and worm-like micelles to spherical micelles, thus the nonspherical and spherical micelles are of the analogical endocytosis effect for HepG2 tumor cells by the 2nd day, with a further decrease in the difference of the cell viability. Fig. 7b displays the optical microscope images of HepG2 cells cultured with poly(PEG$_{4000}$: CPP : SA) (20 : 20 : 60) micelles with different morphologies at the concentrations of 0.25 and 2.0 mg mL^{-1} for 1 day and 2 days. The results are consistent with the MTT assay. From these images, it can be seen that the general state of cell is the best, and the amount was the most in the rod-like group on the 1st day, suggesting that the rod-like micelles possess the best biocompatibility.

The effect of micelle morphology on cellular uptake

Fig. 8 displays a series of fluorescence images of fibroblast and HepG2 cells treated by DOX·HCl-loaded micelles with rod-like, worm-like and spherical shapes for 0.5, 3 and 6 h, respectively. It can be found that the fluorescence intensity of DOX·HCl inside cells increased as the culture time prolonged. At 6 h, the red fluorescence in cells is very obvious for all the cells treated with micelles. It should be mentioned that the intensity in fibroblast cells is not stronger than that in the HepG2 tumor cells at the same time. The reason may be that the micelles prefer to enter tumor cells. By comparison, the fluorescence intensity of cells treated with spherical micelles is the highest among the three types of micelles, indicating that the spherical micelles are more likely to be taken up by these cells. Most

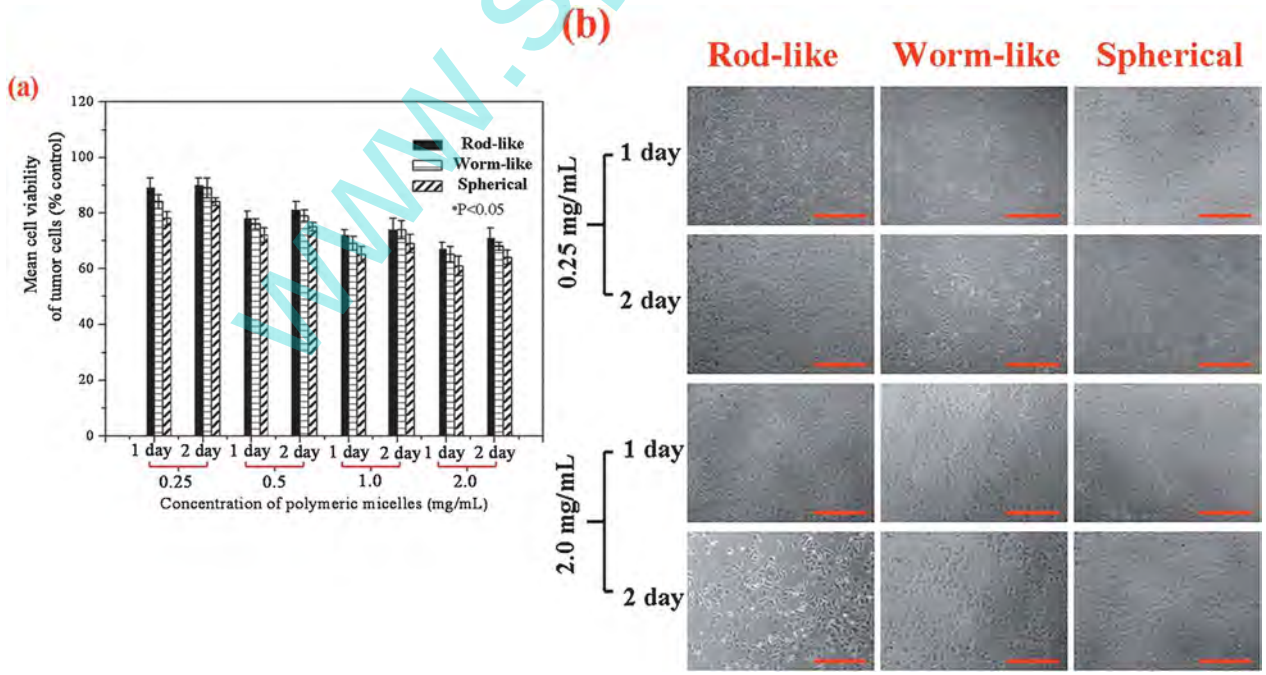

Fig. 7 *In vitro* tumor cell growth inhibition assay (a) and optical microscope images (b) of HepG2 cells cultured with poly(PEG$_{4000}$: CPP : SA) (20 : 20 : 60) micelles with different morphologies at the concentrations of 0.25 and 2.0 mg mL^{-1} for 1 day and 2 days (all scale bars are 50 μm).

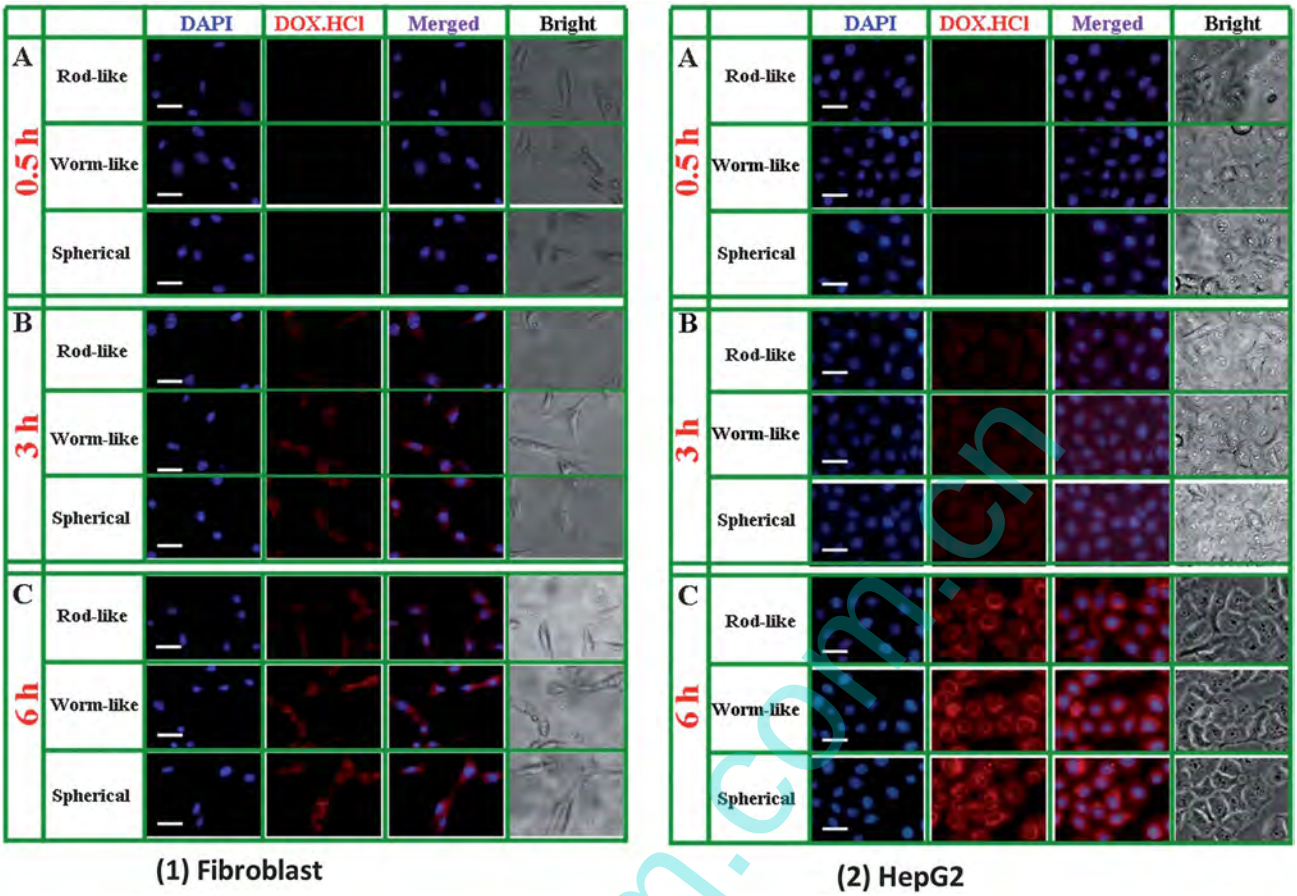

Fig. 8 Fluorescence microscopy images of (1) fibroblast and (2) HepG2 tumor cells incubated with DOX·HCl-loaded micelles (red) of different morphologies for 0.5 h (A), 3 h (B) and 6 h (C), respectively. The scale bars are 40 μm in all the images and cell nuclei stained with DAPI (blue).

micelle drug delivery systems can enter cells through caveolae-mediated endocytosis.[43–45]

The effect of micelle morphology on biodistribution in *in vivo*

Nanocarriers can evidently change *in vivo* biodistribution of the therapeutic drug loaded. The optimum biodistribution improves the bioavailability of drug and diminishes side effects.[46] *In vivo* biodistribution of the DOX·HCl-loaded micelles in normal and tumor tissues is displayed in the typical fluorescence microscopy images at 6 h and 24 h in Fig. 9. Fig. 9A displays that DOX·HCl accumulated in the tumor can be detected clearly in all groups at 6 h. Higher fluorescence intensity could be observed in the groups treated with DOX·HCl-loaded micelles compared with the free DOX·HCl treatment. The highest fluorescence intensity is for the group treated with rod-like micelles. After 24 h the fluorescence intensity in the tumor sites shows a decrease to some extent in all groups, especially for the free DOX·HCl treatment, whereas the fluorescence intensity in the group treated with rod-like micelles is still the highest, maybe because the rod-like carrier has the capability of circulating longer than the spherical vector. The rod-like carrier is more likely to be taken up or eliminated by cells of the immune system, and more readily to accumulate in the tumor site than the normal tissues because of the enhanced permeation and retention (EPR) effect.[16,47]

To analyze the *in vivo* biodistribution of free DOX·HCl and the three types of DOX·HCl-loaded micelles quantitatively, UV-vis spectrophotometry was employed to measure the content of DOX·HCl in normal and tumor tissues. Biodistribution of free DOX·HCl and DOX·HCl-loaded micelles of different morphologies at 6 h and 24 h is shown in Fig. 9B. It must be pointed out that the DOX·HCl level in both tumor and normal tissues decreased with the time. As shown in Fig. 9B, the content of free DOX·HCl is much lower than that of DOX·HCl-loaded micelles at the tumor site, and free DOX·HCl in normal tissues is more than these micelles. For the three types of micelles, the longer the micelles are, the more the DOX·HCl accumulates in the tumor site, due to the tumor-featured EPR effect. It is also demonstrated that the DOX·HCl-loaded micelles can circulate *in vivo* for a longer time, especially for the rod-like micelles. The result is in agreement with the report by Discher *et. al.*[16] The longer circulation time may be due to the fact that the formulation of micelles can protect DOX·HCl and prevent it from being taken up by the RES and macrophages.[48] In addition, we also find that the content of the DOX·HCl-loaded micelles are prone to accumulate in the liver and spleen with the time increasing, which is beneficial to eccrisis. The results suggest

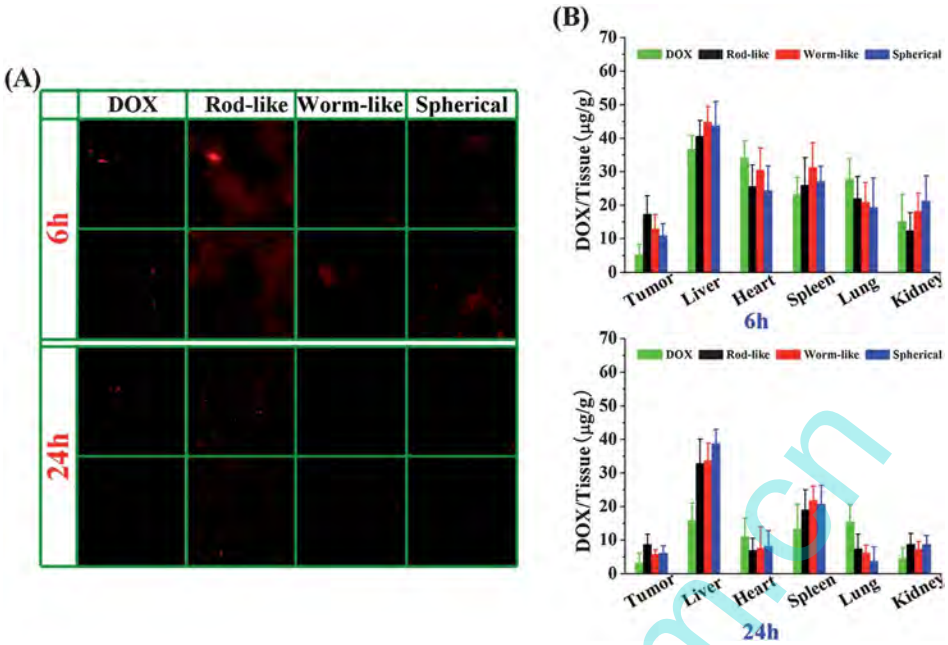

Fig. 9 (A) Fluorescence microscopy images and (B) biodistribution profiles of DOX·HCl in tumor and normal tissues from mice with 4T1 breast tumors after intravenous administration of free DOX·HCl and rod-like, worm-like and spherical DOX·HCl-loaded micelles at an equivalent DOX·HCl dose of 5 mg kg^{-1} at the time of 6 h and 24 h.

that the DOX·HCl-loaded micelles have lower toxicity to normal tissues than free DOX·HCl.

Conclusions

To the best of our knowledge, there are few comprehensive and systematic reports about the effects of different factors on the morphology of polymeric micelles, especially the morphological transition, prepared with PEG-based ether-anhydride terpolymers. In this study, micelles with various morphologies (rod-like, worm-like and spherical) formed from the amphiphilic poly(PEG : CPP : SA) terpolymers are prepared. The morphological transition of the micelles can be controlled by changing PEG chain length, the hydrophilic–hydrophobic segment ratio, concentration of polymer and the environmental temperature due to the entropy change and free energy balance. As drug nanocarriers, the longest rod-like micelles possess the highest drug-loading efficiency, which could be contributed to their large core volume and large area of the aggregation cavity. MTT assay reveals that micelle morphology affects the cell viability of HepG2, and rod-like micelles exhibit the best biocompatibility. The fluorescence microscopy images of tumor tissues suggest that rod-like micelles have the capability of circulating longer than other vectors which are easier to be eliminated by cells of the immune system. Therefore, the micellar shape is very important when the micelles are selected as drug carriers in nanomedicine.

Acknowledgements

This work was partially supported by the National Basic Research Program of China (973 Program, 2012CB933602), the National Natural Science Foundation of China (no. 30970723 and 51173150), the National Key Project of Scientific and Technical Supporting Programs Funded by MSTC (2012BAI17B06) and the Fundamental Research Funds for the Central Universities (SWJTU11ZT10).

References

1 J. P. Darrin, Z. Y. Chen, H. G. Cui, K. Hales, K. Qi, L. Karen and T. Wooley, *Science*, 2004, **306**, 94–97.
2 Y. Kakizawa and K. Kataoka, *Adv. Drug Delivery Rev.*, 2002, **54**, 203–222.
3 A. Rosler, G. W. Vandermeulen and H. A. Klok, *Adv. Drug Delivery Rev.*, 2001, **53**, 95–108.
4 H. M. Aliabadi and A. Lavasanifar, *Expert Opin. Drug Delivery*, 2006, **3**, 139–162.
5 M. L. Forrest, C. Y. Won, A. W. Malick and G. S. Kwon, *J. Controlled Release*, 2006, **110**, 370–377.
6 H. Maeda, J. Wu, T. Sawa, Y. Matsumura and K. Hori, *J. Controlled Release*, 2000, **65**, 271–284.
7 V. Hugouvieux, M. A. V. Axelos and M. Kolb, *Soft Matter*, 2011, **7**, 2580–2591.
8 C. Monica, J. K. Branco and P. S. Joel, *Acta Biomater.*, 2009, **5**, 817–831.
9 Y. Dong and S. Feng, *Biomaterials*, 2004, **25**, 2843–2849.
10 A. Mahmud, X. B. Xiong and A. Lavasanifar, *Macromolecules*, 2006, **39**, 9419–9428.
11 O. Soga, N. C. Van, A. Ramzi, T. Visser, F. Soulimani and P. M. Frederik, *Langmuir*, 2004, **20**, 9388–9395.
12 A. Harada and K. Kataoka, *Prog. Polym. Sci.*, 2006, **31**, 949–982.

13 C. Irene, L. Reynhout, J. Jeroen, M. Cornelissen and J. M. Roeland, *J. Am. Chem. Soc.*, 2007, **129**, 2327–2332.
14 J. Sumeet and S. B. Frank, *Science*, 2003, **300**, 460–464.
15 P. D. Haimer, A. J. Engler, R. Parthasarathy and D. E. Discher, *Biomacromolecules*, 2004, **5**, 1714–1719.
16 Y. Geng, P. Dalhaimer, S. Cai, R. Tsai, M. Tewari, T. Minko and D. Discher, *Nat. Nanotechnol.*, 2007, **2**, 249–255.
17 S. S. Cai, K. Vijayan, D. Cheng, E. M. Lima and D. E. Discher, *Pharm. Res.*, 2007, **24**, 2099–2109.
18 G. Sharma, D. T. Valenta, Y. Altman, S. Harvey, H. Xie, S. Mitragotri and J. W. Smith, *J. Controlled Release*, 2010, **147**, 408–412.
19 S. Y. Lin, W. H. Hsu, J. M. Lo, H. C. Tsai and G. H. Hsiue, *J. Controlled Release*, 2011, **154**, 84–92.
20 A. H. Lee and K. T. Oh, *Bull. Korean Chem. Soc.*, 2010, **31**, 2265–2271.
21 N. Fairley, B. Hoang and C. Allen, *Biomacromolecules*, 2008, **9**, 2283–2291.
22 Z. L. Lei and L. Zhang, *Colloids Surf., A*, 2008, **312**, 166–171.
23 Y. Zhang, X. Xiao, J. J. Zhou, L. Wang, Z. B. Li, L. Li, L. Q. Shi and C. M. Chan, *Polymer*, 2009, **50**, 6166–6171.
24 Z. X. Du, J. T. Xu and Z. Q. Fan, *Macromolecules*, 2007, **40**, 7633–7637.
25 Y. P. Wang, H. P. Xu and X. Zhang, *Adv. Mater.*, 2009, **21**, 2849–2864.
26 H. G. Cui, Z. Y. Chen, S. Zhong, L. Karen and D. J. Wooley, *Science*, 2007, **317**, 647–650.
27 T. Kawaguchi, T. Honda, M. Nishihara, M. Yokoyama and T. Yamamoto, *J. Controlled Release*, 2009, **136**, 240–246.
28 J. Fu, J. Fiegel and J. Hanes, *Macromolecules*, 2004, **37**, 7174–7180.
29 N. Kumar, R. Langer and J. Abraham, *Adv. Drug Delivery Rev.*, 2002, **54**, 889–910.
30 N. Zhang and S. R. Guo, *J. Polym. Sci., Part A: Polym. Chem.*, 2006, **44**, 1271–1278.
31 L. Zhang and A. Eisenberg, *Science*, 1995, **268**, 1728–1731.
32 A. J. Zhao, Q. Zhou, T. Chen, J. Weng and S. B. Zhou, *J. Appl. Polym. Sci.*, 2010, **118**, 3576–3585.
33 L. G. Lei, J. F. Gohy, N. Willet, J. X. Zhang, R. Jerome and S. Varshney, *Polymer*, 2006, **47**, 2723–2727.
34 Y. Liu, Z. X. Zhao and J. Wei, *J. Colloid Interface Sci.*, 2007, **314**, 470–477.
35 T. Vilgis and A. Halperin, *Macromolecules*, 1991, **24**, 2090–2095.
36 H. W. Shen and A. Eisenberg, *J. Phys. Chem. B*, 1990, **103**, 9473–9487.
37 L. Desbaumes and A. Eisenberg, *Langmuir*, 1999, **15**, 36–38.
38 A. J. Zhao, S. B. Zhou, Q. Zhou and T. Chen, *Pharm. Res.*, 2010, **27**, 1627–1643.
39 Y. Tang and J. Singh, *Int. J. Pharm.*, 2009, **365**, 34–43.
40 J. P. Mata, P. R. Majhi, C. Guo, H. Z. Liu and P. Bahadur, *J. Colloid Interface Sci.*, 2005, **292**, 548–556.
41 L. Yu, G. Tao, C. Huan and J. D. Ding, *J. Polym. Sci., Part A: Polym. Chem.*, 2007, **45**, 1122–1133.
42 Y. Geng, E. Dennis and C. R. Discher, *Polymer*, 2006, **47**, 2519–2525.
43 G. Sahay, D. Y. Alakhova and A. V. Kabanov, *J. Controlled Release*, 2010, **145**, 182–195.
44 F. Danhier, O. Feron and V. Préat, *J. Controlled Release*, 2010, **148**, 135–146.
45 G. Sahay, J. O. Kim, A. V. Kabanov and T. K. Bronich, *Biomaterials*, 2010, **31**, 923–933.
46 S. M. Moghimi, A. C. Hunter and J. C. Murray, *Pharmacol. Rev.*, 2001, **53**, 283–318.
47 D. A. Christian, S. Cai, O. B. Garbuzenko, T. Harada, A. L. Zajac and T. Minko, *Mol. Pharmaceutics*, 2009, **6**, 1343–1352.
48 S. Q. Liu, N. Wiradharma, S. J. Gao, Y. W. Tong and Y. Y. Yang, *Biomaterials*, 2007, **28**, 1423–1433.